Expression and Structural Characterization of the Recombinant Human Doppel Protein[†,‡]

Ke Lu,[§,||] Wen Wang,[§,||] Zhiliang Xie,[§] Boon-Seng Wong,[§] Ruliang Li,[§] Robert B. Petersen,[§] Man-Sun Sy,[§] and Shu G. Chen*[,§,⊥]

Institute of Pathology and Mass Spectrometry Core Facility, Case Western Reserve University, 2085 Adelbert Road, Cleveland, Ohio 44106

Received July 5, 2000; Revised Manuscript Received September 1, 2000

ABSTRACT: The doppel protein (Dpl) is a newly recognized prion protein (PrP)-like molecule encoded by a novel gene locus, *prnd*, located on the same chromosome as the PrP gene. To study the structural features of Dpl, we have expressed recombinant human Dpl corresponding to the putative mature protein domain (residues 24−152) in *Escherichia coli*. The primary structure of the recombinant Dpl 24−152 was characterized using gel electrophoresis, N-terminal Edman sequencing, matrix-assisted laser desorption ionization mass spectrometry, and electrospray ionization mass spectrometry. Dpl 24−152 was shown to contain two disulfide bonds (Cys94−Cys145 and Cys108−Cys140). The secondary structure of Dpl was analyzed using far-UV circular dichroism spectroscopy. Dpl 24−152 was found to be an α-helical protein having a high helical content (40%). Dpl 24−152 exhibited characteristics of a thermodynamically stable protein that undergoes reversible and cooperative thermal denaturation. In addition, Dpl was found to be soluble and sensitive to proteinase K digestion. Therefore, Dpl 24−152 possesses biochemical properties similar to those of recombinant PrP. This study provides knowledge about the molecular features of human Dpl that will be useful in further investigation into its normal function and the role it may play in neurodegenerative diseases.

Doppel (Dpl)[1] (downstream, prion protein-like) was recently identified in mammals (*1*). It is encoded within a single exon of a novel gene, *prnd*, located 16 kb downstream of the mouse PrP gene and 27 kb downstream of the human PrP gene. The sequence of Dpl is notably homologous to that of PrP. Dpl is associated with neurodegeneration when ectopically expressed in several lines of transgenic mice (*1*). The discovery of Dpl suggests, that in addition to PrP, other PrP-related proteins may contribute to the pathogenesis of neurodegenerative diseases.

According to the "protein only" hypothesis, prion diseases are disorders of PrP conformation (*2*). PrP normally adopts a highly α-helical globular structure in its native, cellular form (PrP^C), which can be converted into the β-sheet rich, protease-resistant pathogenic isoform (PrP^{Sc} or PrP^{res}) by a post-translational process. However, the mechanism by which PrP^{Sc} causes prion diseases and the physiological function of PrP^C remain uncertain. It has been shown that the expression of PrP^C is highly regulated during cellular differentiation and embryonic development (*3*, *4*). There is also evidence that PrP^C binds copper ions via its N-terminal octapeptide repeat region (*5*−*7*), suggesting that PrP may be involved in a copper-mediated cellular process. However, the first two lines of PrP knockout mice were viable and exhibited no obvious developmental abnormality (*8*, *9*). In contrast, two new lines of PrP knockout mice that involved different gene ablation strategies showed late-onset ataxia and Purkinje cell loss in cerebellum (*1*, *10*). The latter observation was attributed to the ectopic overexpression of Dpl caused by unintended perturbation of the promoter region during targeted disruption of the PrP gene (*1*). Therefore, Dpl may play a role in neurodegeneration of the central nervous system. One possibility is that Dpl and PrP share essential biochemical properties and thus have similar functions. Alternatively, Dpl may represent a protein that is evolutionarily diverged from PrP with newly acquired properties. In either case, examining the structural features of Dpl may provide valuable insight into the biology of Dpl.

The translated sequence of human doppel consists of 176 residues. At the amino acid sequence level, Dpl and PrP share

[†] This work was supported by grants from the National Institutes of Health (Grants AG14359 and AG15162). Partial funding for the Mass Spectrometry Core Facility was provided by the Ireland Cancer Center, Case Western Reserve University, and University Hospitals of Cleveland.

[‡] Part of this work was presented at the Concerted Action Meeting on Human Transmissible Spongiform Encephalopathy, May 27-30, 2000, Baden, Austria.

* To whom correspondence should be addressed: Institute of Pathology, Case Western Reserve University, 2085 Adelbert Road, Cleveland, OH 44106. Tel.: (216) 368−8925. Fax: (216) 368−2546. E-mail: sxc59@po.cwru.edu.

[§] Institute of Pathology.

[||] These authors contributed equally to this study.

[⊥] Mass Spectrometry Core Facility.

[1] Abbreviations: Dpl, doppel protein; PrP, prion protein; GPI, glycophosphatidylinositol; PCR, polymerase chain reaction; EK, enterokinase; IPTG, isopropyl β-D-galactopyranoside; GndHCl, guanidine hydrochloride; Ni−NTA, nickel−nitrilotriacetic acid; SDS−PAGE, sodium dodecyl sulfate−polyacrylamide gel electrophoresis; MALDI, matrix-assisted laser desorption ionization; ESI, electrospray ionization; MS, mass spectrometry; HPLC, high-performance liquid chromatography; CD, circular dichroism; PK, proteinase K.

10.1021/bi001523m CCC: $19.00
Published on Web 10/11/2000

similarities as well as differences. The N- and C-terminal regions of Dpl and PrP are conserved to a large extent, including an N-terminal signal sequence and a C-terminal hydrophobic sequence for glycophosphatidylinositol (GPI) anchor attachment. Both of the mature proteins contain consensus motifs for Asn-linked glycosylation. However, Dpl lacks sequences homologous to the PrP regions containing the copper-binding octapeptide repeats and the highly conserved neurotoxic segment (PrP 106−126). In addition, the overall degree of sequence homology between the two proteins is only about 25%. Therefore, experimental data are needed to clarify the molecular and biochemical features of Dpl in comparison to PrP.

We have now expressed recombinant human Dpl corresponding to its putative mature protein domain (residues 24−152) in *Escherichia coli* and characterized Dpl in terms of its primary and secondary structures, intrinsic protein stability, and protease sensitivity.

MATERIALS AND METHODS

Plasmid Construction. Standard cloning procedures were used (*11*). The open reading frame of the human *PRND* gene (GenBank accession number AF106918) corresponding to the putative mature Dpl inclusive of residues 24−152 was amplified by polymerase chain reaction (PCR) using a human genomic DNA template. Two oligonucleotide primers [5′-GACGACGACAAGATGGTCCAGACGAGGGGCA-3′ (forward sequence) and 5′-GAGGAGAAGCCCGGTTTAGCCCCTCTCCAACCAAAACT-3′ (reverse sequence)] with the ligation-independent cloning sites were synthesized (Operon). Using the Expand High Fidelity PCR system (Boehringer Mannheim), PCR was performed for 30 cycles (94 °C for 1 min, 55 °C for 2 min, and 72 °C for 3 min) with final extension at 72 °C for 10 min in 100 μL containing 50 pmol of primers, 750 ng of DNA template, and dNTPs (400 μM each). The PCR product (420 bp) was purified on a 1.2% agarose gel and recovered using the QIAquick Gel Extraction Kit (Qiagen). The purified PCR fragment was cloned into the pET-30 LIC/EK vector using the ligation-independent cloning method according to the manufacturer's instruction (Novagen). The resulting construct is under the control of both the T7 promoter and lac operator, and encodes an N-terminal 43-amino acid fusion peptide that includes a polyhistidine tag and an engineered enterokinase (EK) cleavage site, followed by an additional methionine fused to Dpl 24−152. The construct was transformed into NovaBlue Singles *E. coli* competent cells (Novagen). Clones containing the construct were identified, and the cDNA insert was completely sequenced using an ABI 377 Prism automated DNA sequencer (Perkin-Elmer) to ensure that no unintended mutations had been introduced. The above strategy yields a recombinant Dpl 24−152 with only one extra residue (M) at the N-terminus after cleavage of the fusion peptide by EK.

Expression and Purification of Dpl 24−152. The recombinant Dpl 24−152/pET30 plasmid was isolated from NovaBlue *E. coli* cells and transformed into the expression host, BL21(DE3) *E. coli* cells (Novagen). Freshly transformed cells were incubated at 37 °C with constant shaking in 3 mL of Luria broth (LB) supplemented with 30 μg/mL kanamycin until the OD_{600} reached 0.6−1.0. The culture was then expanded into 1 L in LB supplemented with 30 μg/mL kanamycin. When the expanded culture reached an OD_{600} of 0.6, the expression of recombinant polyhistidine-tagged Dpl was induced by adding isopropyl β-D-galactopyranoside (IPTG) to a final concentration of 1 mM. The culture was harvested 8−12 h after induction, centrifuged, and resuspended in 24 mL of buffer A [6 M guanidine hydrochloride (GndHCl), 10 mM Tris-HCl, 50 mM Na_2HPO_4, 100 mM NaCl, and 10 mM reduced glutathione (pH 8.0)], supplemented with protease inhibitors (3 mM PMSF, 10 μg/mL leupeptin, and 0.1 mM apoprotinin). Solubilized proteins were released by four cycles of freezing (dry ice) and thawing (sonication at 4−10 °C). After centrifugation, the soluble fraction was mixed with 8 mL of nickel−nitrilotriacetic acid (Ni−NTA) agarose (Qiagen) equilibrated in buffer A. After a 30 min incubation, the resin was poured into a column and washed with 30 mL of buffer A. On-column oxidative refolding of the immobilized polyhistidine tag-fused Dpl was achieved by applying a 60 mL gradient of buffer A to buffer B [10 mM Tris-HCl and 50 mM Na_2HPO_4 (pH 8.0)] at a flow speed of 0.5 mL/min, followed by washing with 10 mL of buffer B. The polypeptide was eluted in 24 mL of buffer E [50 mM NaH_2PO_4 and 500 mM imidazole (pH 6.0)]. After the resin had been washed with buffer A, oxidative refolding and imidazole elution were repeated to obtain a second batch of soluble protein. The combined fractions were treated with 1 unit/mL recombinant EK (Novagen) to remove the N-terminal tag from the Dpl-containing fusion protein. The resulting Dpl 24−152 was separated from EK and the N-terminal tag by cation exchange chromatography on CM resin (Sigma) equilibrated with buffer F [10 mM sodium phosphate (pH 6.0)]. Dpl 24−152 was eluted at 150−250 mM NaCl using a gradient of 0−500 mM NaCl in buffer F at a flow rate of 0.5 mL/min. Fractions containing Dpl were identified by SDS−PAGE (16% gel, Novex) and Coomassie blue staining, pooled, concentrated by ultrafiltration (10 kDa cutoff membrane, Amicon), and dialyzed against buffer F. The concentration of Dpl 24−152 was determined by UV absorbance using a molar extinction coefficient ϵ_{280} of 28 120 M^{-1} cm^{-1}.

N-Terminal Protein Sequencing. Proteins separated by SDS−PAGE were electroblotted onto a Problott sequencing membrane (Perkin-Elmer). The protein band was excised and subjected to Edman degradation for 10−15 cycles on an Applied Biosystems 494 Procise instrument.

Matrix-Assisted Laser Desorption Ionization Mass Spectrometry (*MALDI-MS*). The MALDI-MS instrument was equipped with a pulsed nitrogen laser source (λ = 337 nm) and used at an acceleration voltage of 28 kV operated in the linear mode (Voyager Biospectrometry Workstation, PerSeptive Biosystems, Framingham, MA). Samples were mixed with an equal volume of a saturated matrix solution (α-cyano-4-hydroxycinnamic acid for peptides and sinapinic acid for proteins in 60% acetonitrile and 0.3% trifluoroacetic acid). One microliter of the mixture was applied onto the laser target probe and was air-dried before being introduced into the mass spectrometer. Singly protonated ions were most frequently observed, allowing for simple assignment of molecular species. Between 100 and 200 spectra were obtained for each sample. The spectra were averaged and analyzed using the GRAMS software on the instrument. The instrument was calibrated using a mixture of standard

peptides. A mass accuracy of 0.03−0.05% was routinely obtained.

Electrospray Ionization Mass Spectrometry (ESI-MS). ESI-MS was performed on an ion trap LCQ mass spectrometer (Finnigan) using nitrogen as the sheath gas. The mass spectrometer was equipped with an ESI needle with an ion-spray voltage set at 3000 V. Samples were introduced either by direct infusion at 5 μL/min or through on-line reverse phase high-performance liquid chromatography (HPLC) on a Michrom BioResources microbore column (C18, 5 μm, 200 Å, 1.0 mm × 150 mm) at 50 μL/min using a gradient of 0 to 65% acetonitrile containing 0.05% formic acid and 0.005% trifluoroacetic acid. The spectra were acquired in the full scan mode using the Xcalibur control software. The *m*/*z* range of the instrument was 0−2000. Unlike MALDI, ESI resulted in the formation of multiple protonated ions. Assignment of multiple charged ions to their original molecules was assisted by computer-aided deconvolution, which transforms *m*/*z* values to M_r values using BioWorks software (Finnigan). The mass accuracy was usually better than 0.005%.

Peptide Mass Mapping. Dpl 24−152 (20 μg) was incubated at 37 °C for 4 h with sequencing-grade endoproteinase Lys-C (Boehringer Mannheim) at a ratio of 20:1 in 20 mM sodium phosphate (pH 7.0). The digestion products were analyzed using either MALDI-MS without separation or ESI-MS following on-line HPLC.

Circular Dichroism (CD) Spectroscopy. Far-UV CD spectra of Dpl [10−20 μM Dpl in 10 mM potassium phosphate (pH 6.0)] were recorded on a Jasco 810 spectropolarimeter between 185 and 250 nm using a 0.1 cm cuvette, and near-UV CD spectra [100 μM Dpl in 10 mM potassium phosphate (pH 6.0)] were recorded between 250 and 350 nm using a 1 cm cuvette. Ellipticity was measured every 1 s with a response time of 1 s and a bandwidth of 1 nm. Between four and eight scans were collected and averaged. The α-helical content was estimated using the self-consistent method (*12*). For thermal unfolding, ellipticity at 222 nm was monitored over the temperature range of 20−85 °C in increments of 0.2 °C with a gradient of 1 °C/min. The CD data were fit to a two-state model with six parameters to obtain T_m, the midpoint of transition temperature, and ΔH_m, the enthalpy of unfolding at T_m, using the KaleidaGraph program (Synergy Software). Fractions of unfolded Dpl were calculated by normalizing the CD intensities at different temperatures to those obtained at 20 °C. Reversibility was checked by measuring the CD after the heated samples were cooled to 20 °C.

Assays for Protein Solubility and Protease Sensitivity. The solubility of Dpl was tested by centrifuging Dpl (0.2 mg/mL) in a buffer containing 150 mM NaCl and 10 mM Tris (pH 7.0) at 20000*g* for 1 h at 4 °C. The supernatant was transferred into a new tube. The remaining sample in the original tube was considered to be the pellet fraction, which was then resuspended in the same buffer. In a separate experiment, 0.5% Triton X-100 and 0.5% sodium deoxycholate were present in the buffer. The supernatant and pellet fractions were analyzed for the presence of Dpl by SDS−PAGE. The protease sensitivity of both recombinant Dpl and PrP was performed using a standard protocol, as described previously (*13*, *14*). Proteins (0.2 mg/mL) were digested with proteinase K (PK) at 37 °C for 1 h in the digestion buffer containing 1 mM EDTA, 0.05% Nonidet P-40, 0.05% sodium deoxycholate, and 10 mM sodium phosphate (pH 7.0). PK was used at concentrations of 1, 2, 5, 10, 20, and 50 μg/mL. The digestion was terminated by the addition of 5 mM phenylmethanesulfonyl fluoride. The digest was boiled in SDS sample buffer and analyzed by SDS−PAGE.

Antibody Production and Western Blotting. A peptide (CDIDFGAEGNRYYAANYWQFPD) corresponding to mouse Dpl residues 68−88 was synthesized by Fmoc chemistry. The peptide is 95% homologous to the human sequence (substitution of A for E at position 81). The peptide was conjugated to maleimide-activated KLH via a free sulfhydryl group (Princeton Biotechnology) and mixed with complete Freund's adjunct prior to subcutaneous injection into FVB mice (Jackson Laboratory). The antisera were obtained after boosting three times at weekly intervals. Western blotting was performed as previously described (*15*).

RESULTS

Expression and Purification of Recombinant Human Dpl. As shown by molecular modeling (*1*), the human Dpl precursor (residues 1−176) is predicted to include an N-terminal signal peptide sequence (residue 1−23) and a hydrophobic C-terminal sequence (residues 153−176) for attachment of a GPI anchor. Both of these segments are expected to be removed in the mature protein, like PrP and other GPI-anchored proteins (*16*, *17*). For that reason, the putative mature human Dpl protein corresponding to residues 24−152 was chosen for expression as a recombinant protein in *E. coli* cells. A high-yield expression system under the control of T7 and lac operator (pET vector), which has been successful in expressing the recombinant PrP (*14*), was employed to obtain large quantities of Dpl for structural studies.

Dpl was cloned into the pET-30 LIC/EK vector and expressed as a fusion protein containing an N-terminal tag with polyhistidine residues followed by an EK cleavage site. This cloning strategy minimizes the incorporation of vector coding sequence into Dpl 24−152, which will contain only an extra methionine residue at the N-terminus. As was the case for recombinant PrP (*14*, *18*), the Dpl fusion protein was recovered in inclusion bodies in the cytoplasm of *E. coli* cells. The inclusion bodies were extracted in a buffer containing GndHCl and reduced glutathione for efficient solubilization of the proteins and to prevent the formation of intermolecular disulfide bonds. The Dpl fusion protein was bound through its N-terminal polyhistidine tail to Ni−NTA resin, which allowed for the removal of most other proteins. To obtain correctly folded Dpl, oxidative refolding was performed on the immobilized protein by applying a decreasing GndHCl/glutathione gradient (*18*). The refolded Dpl fusion protein was eluted from the Ni−NTA resin by step elution using imidazole at concentrations of >200 mM. The N-terminal fusion tag was subsequently removed by cleavage using recombinant EK. The resulting Dpl 24−152 was further purified by cation exchange chromatography. As shown in Figure 1, these purification steps resulted in the recovery of highly purified fractions of Dpl 24−152. A yield of 3−5 mg of Dpl 24−152 per liter of culture was obtained, with a purity of >95% as judged by staining of gels using Coomassie blue (Figure 1), and by HPLC and free-zone capillary electrophoresis (data not shown).

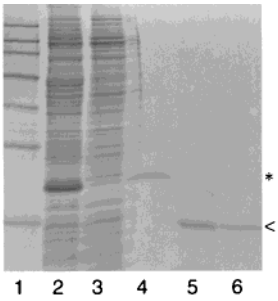

FIGURE 1: Expression of recombinant Dpl 24−152. Proteins were extracted during each purification step and were separated by SDS−PAGE. An equivalent of about 1/1000 fraction of materials was loaded for each lane of 16% gels: lane 1, molecular size markers (from bottom to top) of 15, 25, 35, 50, 75, 100, and 150 kDa; lane 2, initial extract of *E. coli* cells induced with IPTG and used for subsequent purification; lane 3, extract of uninduced *E. coli* cells; lane 4, pooled fractions eluted from Ni−NTA resin; lane 5, fractions after subsequent treatment with EK; and lane 6, pooled fractions from cation exchange chromatography. The positions of the Dpl-containing fusion protein (*) and Dpl 24−152 (<) are indicated on the right.

Primary Structure of Dpl. N-Terminal sequencing by automated Edman degradation of purified Dpl 24−152 identified the first 11 amino acid residues with a single expected sequence of MVQTRGIKHRI (Table 1). To verify that the entire Dpl 24−152 polypeptide backbone was correctly made, mass spectrometric measurements were performed. MALDI-MS showed that Dpl 24−152 was detected as a singly protonated form at *m*/*z* 14 953 and a doubly protonated form at *m*/*z* of 7478, corresponding to the observed M_r of 14 953 ± 5 (Figure 2A). This value is in close agreement with the theoretical M_r value of 14 954.0 for the Dpl 24−152 polypeptide without considering disulfide bonds. A more precise M_r value was obtained using ESI-MS. The ESI-MS spectrum of purified Dpl 24−152 was dominated by multiple protonated ions with charge states ranging from 8 to 17, derived from a single protein species during ionization (Figure 2B). When deconvoluted, Dpl 24−152 exhibited an M_r value of 14 949.9 ± 0.5 that is 4 Da lower than that expected for the fully reduced Dpl 24−152. This result suggests that all four cysteine residues in Dpl 24−152 are utilized to form two disulfide bonds. The four cysteine residues are located in the C-terminal region of Dpl at residues Cys94, Cys108, Cys140, and Cys145. To identify the exact disulfide bond linkage between these cysteine residues, Dpl 24−152 was digested with sequencing-grade endoproteinase Lys-C and the resulting peptide mixture was analyzed by mass spectrometry. As shown in Figure 3A, the MALDI-MS spectrum of the unseparated products of the Lys-C digest revealed the presence of three linked peptide pairs having [M + H] values of 4773, 5332, and 5801. These values corresponded in mass values to peptide 102−126 linked to peptide 127−143 (calculated [M + H] of the dipeptide of 4774.4), peptide 66−101 linked to peptide 44−

Table 1: N-Terminal Sequence Analysis of Purified Dpl 24−152[a]

cycle number	residue (identified)[b]	residue (expected)	amount (pmol)
1	M	M	36.3
2	V	V	34.6
3	Q	Q	41.6
4	T	T	38.1
5	R	R	36.1
6	G	G	23.2
7	I	I	21.2
8	K	K	12.7
9	H	H	10.4
10	R	R	16.0
11	I	I	9.4

[a] The automated Edman degradation was performed using the ABI 477A sequenator with the initial yield of 60% and the repetitive yield of 85%. [b] This refers to the corresponding amino acid of the phenylthiohydantoin derivative identified in a given cycle.

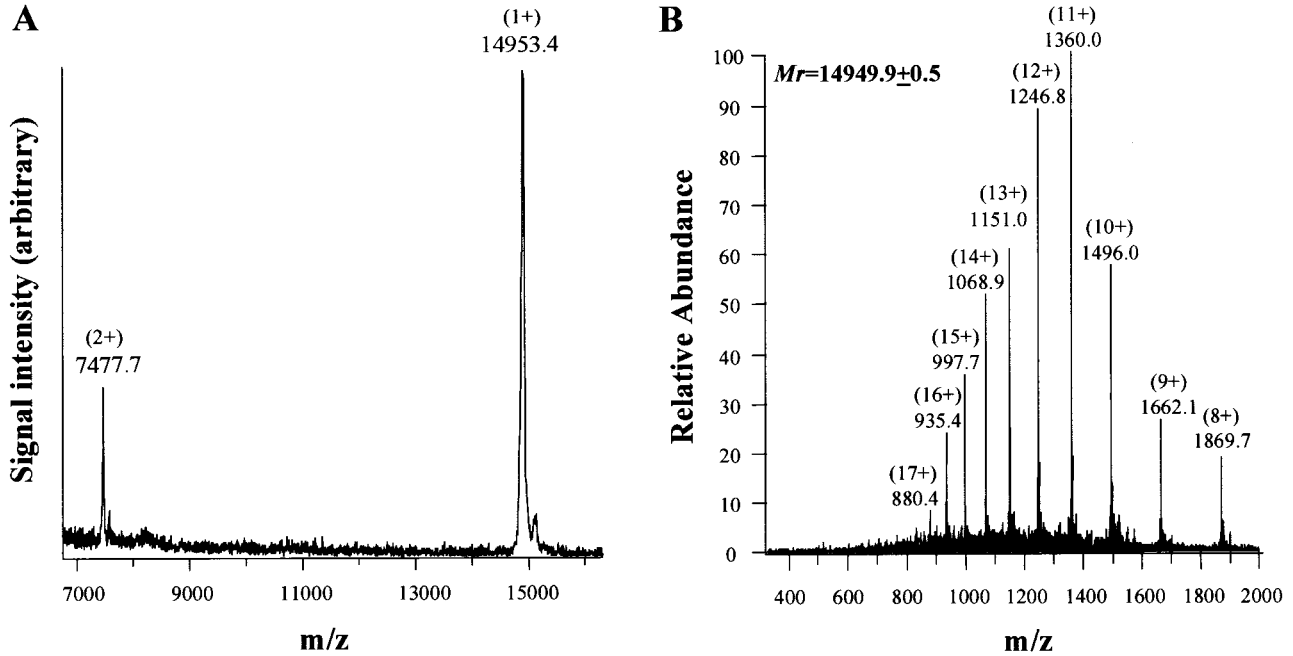

FIGURE 2: Mass spectra of Dpl 24−152. (A) MALDI-MS showed a major molecular ion at *m*/*z* 14 954.3 corresponding to the singly protonated (1+) Dpl 24−152 and an ion at *m*/*z* 7477.7 corresponding to its doubly protonated (2+) form. (B) ESI-MS showed molecular ions containing 8−17 protons (8+ to 17+) at respective *m*/*z* values. Deconvolution of the spectrum resulted in a single species with an M_r value of 14 949.9 ± 0.5.

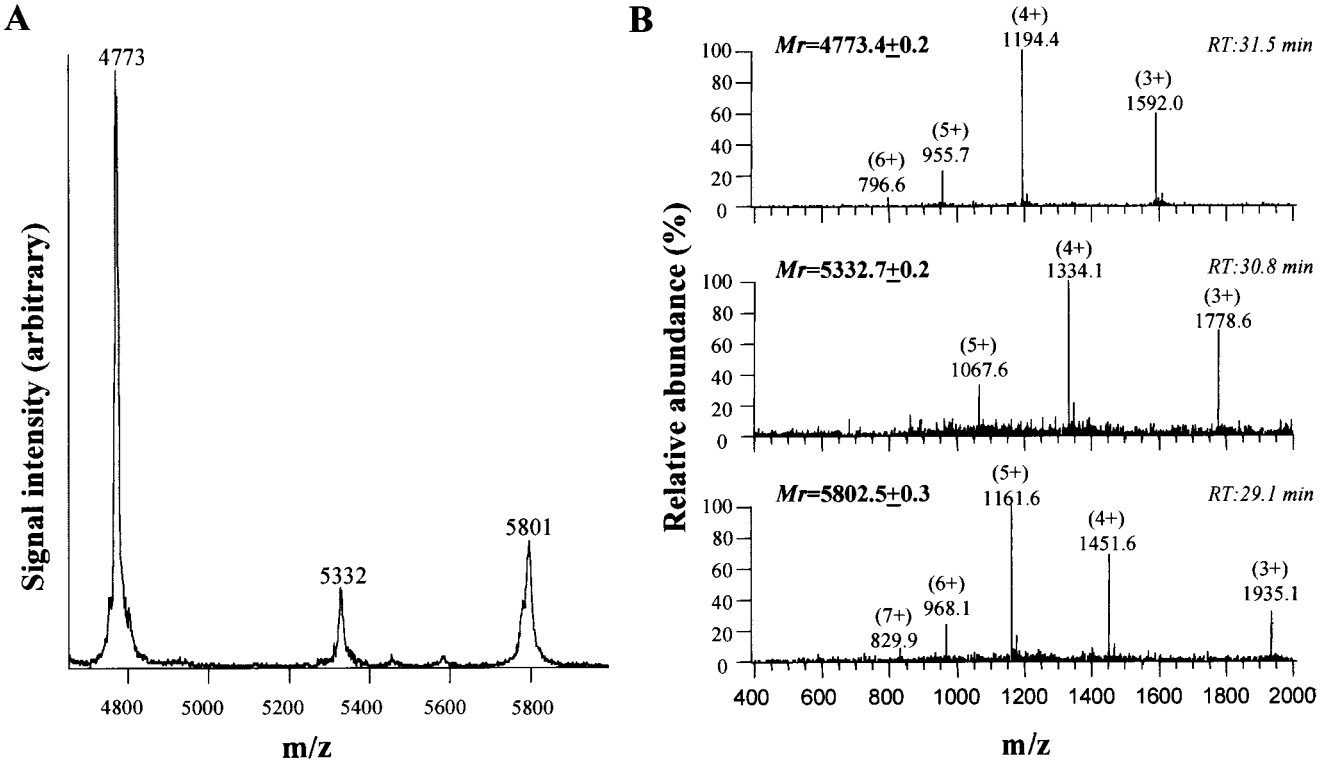

FIGURE 3: Identification of disulfide bonds in Dpl 24−152. Peptides were generated from Lys-C digestion of Dpl 24−152. MALDI-MS of the unseparated digestion mixture (A) showed three singly protonated ions at [M + H] values of 4773, 5332, and 5801 corresponding to three peptide pairs containing disulfide bonds (expected [M + H] values in parentheses): peptide 102−126 with peptide 127−143 (4774.4), peptide 66−102 with peptide 44−152 (5333.8), and peptide 62−101 with peptide 144−152 (5803.3). These three disulfide bond-containing peptide pairs were also detected as multiply protonated ions by ESI-MS after on-line HPLC (B). Deconvolution indicated that the peptide pair with an HPLC retention time (RT) of 31.5 min (upper panel) had an M_r of 4773.4 ± 0.2 corresponding to peptide 102−126 with peptide 127−143; the one with an RT of 30.8 min (middle panel) had an M_r of 5332.7 ± 0.2 corresponding to peptide 66−101 with peptide 44−152, and the one with an RT of 29.1 min (lower panel) had an M_r of 5802.5 ± 0.3 corresponding to peptide 62−101 with peptide 144−152.

Table 2: MS Assignment of Cysteine-Linked Peptides in Lys-C Digest of Dpl 24−152

peptide	cystine pair	M_r (calcd)	M_r (observed, MALDI)	M_r (observed, ESI)
102−126 and 127−143	Cys108−Cys140	4773.4	4772 ± 2	4773.4 ± 0.2
66−101 and 144−152	Cys94−Cys145	5332.8	5331 ± 3	5332.7 ± 0.2
62−101 and 144−152	Cys94−Cys145	5802.3	5800 ± 3	5802.5 ± 0.3

152 (calculated [M + H] of the dipeptide of 5333.8), and peptide 62−101 linked to peptide 144−152 (calculated [M + H] of the dipeptide of 5803.3). These three disulfide bond-linked peptides were also analyzed using on-line HPLC−ESI-MS. The peptide pairs were well resolved by reverse phase HPLC, each with a characteristic ESI-MS spectrum exhibiting multiple protonated molecular ions (Figure 3B). The mass values (M_r) for the three peptide pairs obtained by deconvolution are 4773.4 ± 0.2, 5332.7 ± 0.2, and 5802.5 ± 0.3, respectively. Therefore, the combined peptide mapping data from the unseparated digest mixture using MALDI-MS and from the on-line HPLC-separated peptides using ESI-MS clearly identify two disulfide bonds in Dpl 24−152 (Cys108−Cys140 and Cys94−Cys145) (Table 2). Since no higher molecular oligomers of Dpl 24−152 were observed either on nonreducing polyacrylamide gels (data not shown) or by MALDI-MS and ESI-MS, the results described above suggest that the disulfide bonds in Dpl are formed intramolecularly.

Secondary Structure of Dpl. We used CD to investigate the conformation of Dpl. Dpl 24−152 displayed a maximum at 192 nm and double minima at 208 and 222 nm in the far-UV CD spectrum (Figure 4A), characteristic of the α-helical secondary structure (*12*). The mean residue ellipticities at 208 and 222 nm were −15026 ± 120 and −11965 ± 100 deg cm^2 dmol^{-1}, respectively. The calculated percentage of α-helical content was 40.0 ± 0.5%. Therefore, like recombinant human PrP 23−231 (*18*, *19*), recombinant human Dpl 24−152 is also an α-helical protein having a uniquely folded conformation. In addition, significant CD signals were observed in the near-UV region (Figure 4B), reflecting the strength of aromatic side chain interactions in asymmetric environments. Thus, Dpl 24−152 is likely to have a stable tertiary structure.

The stability, cooperativity, and reversibility during unfolding were examined by monitoring the CD signal at 222 nm after thermal denaturation. The effect of temperature on the α-helical structure of Dpl 24−152 was first noticeable beginning at 45 °C, followed by further loss of secondary structure at higher temperatures and reaching a plateau at about 75 °C (Figure 5A). The cooperativity of the thermal transition was demonstrated by the sigmoidal profile, an indication of native-like packing. Thermal unfolding of Dpl 24−152 was found to be reversible since its original α-helical structure was fully recovered after denaturation when the sample was cooled to 20 °C from 85 °C (Figure 5B). This type of thermodynamic behavior can be best explained by

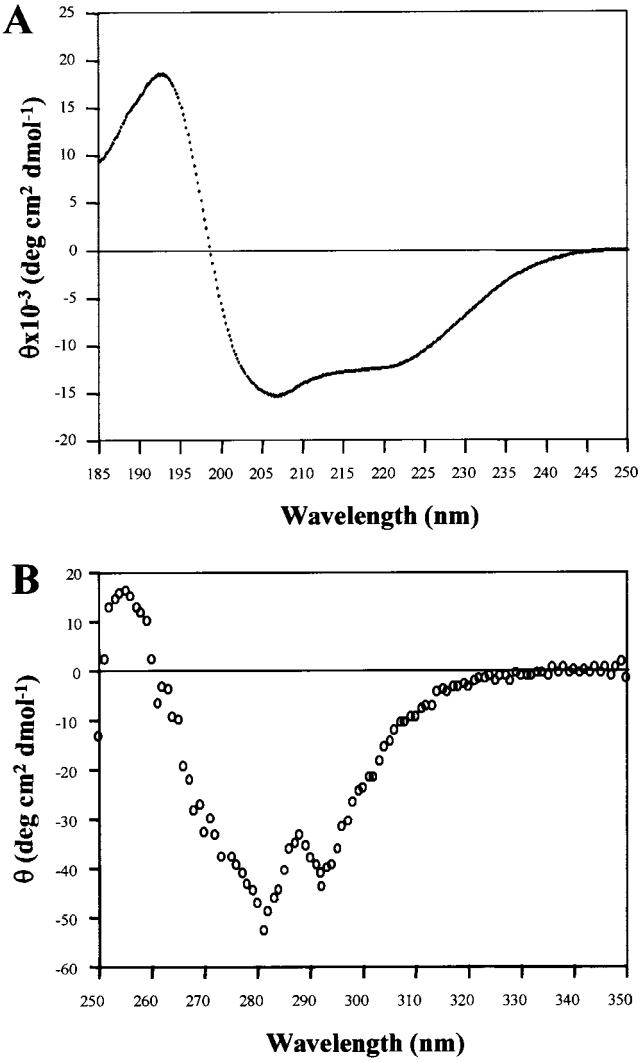

FIGURE 4: CD analysis of Dpl 24−152. Far-UV CD (A) and near-UV CD (B) spectra were recorded in 10 mM potassium phosphate (pH 6.0) at protein concentrations of 12 and 100 μM, respectively.

the two-state unfolding model (*20*). The estimated T_m was 58.3 ± 0.3 °C, and ΔH_m was 194 ± 8 kJ/mol. Either recombinant human PrP 23−231 (*19*) or PrP 90−231 (*21*) was shown previously to undergo cooperative and reversible thermal transition.

Solubility and Protease Sensitivity. Previous studies have shown that recombinant PrP is soluble in its native α-helical conformation, but becomes insoluble and resistant to PK digestion when PrP forms significant β-sheet structure at low pH and in the presence of salt (*14*). We, therefore, examined the solution solubility and protease sensitivity of Dpl. Figure 6 shows that following centrifugation, Dpl 24−152 was recovered in the supernatant either in the absence or in the presence of detergents, suggesting that Dpl was soluble in aqueous solutions at neutral pH. No aggregation was observed even when Dpl was exposed to ambient temperature for a prolonged period of time (>1 week, data not shown). Treatment of Dpl with 5 μg/mL PK for 60 min resulted in complete protein degradation (Figure 7A). When tested under the same conditions, the α-helical rich, recombinant human PrP 23−231 was also degraded at similar PK concentrations (Figure 7B). Therefore, like recombinant PrP 23−231, Dpl 24−152 is sensitive to degradation by PK.

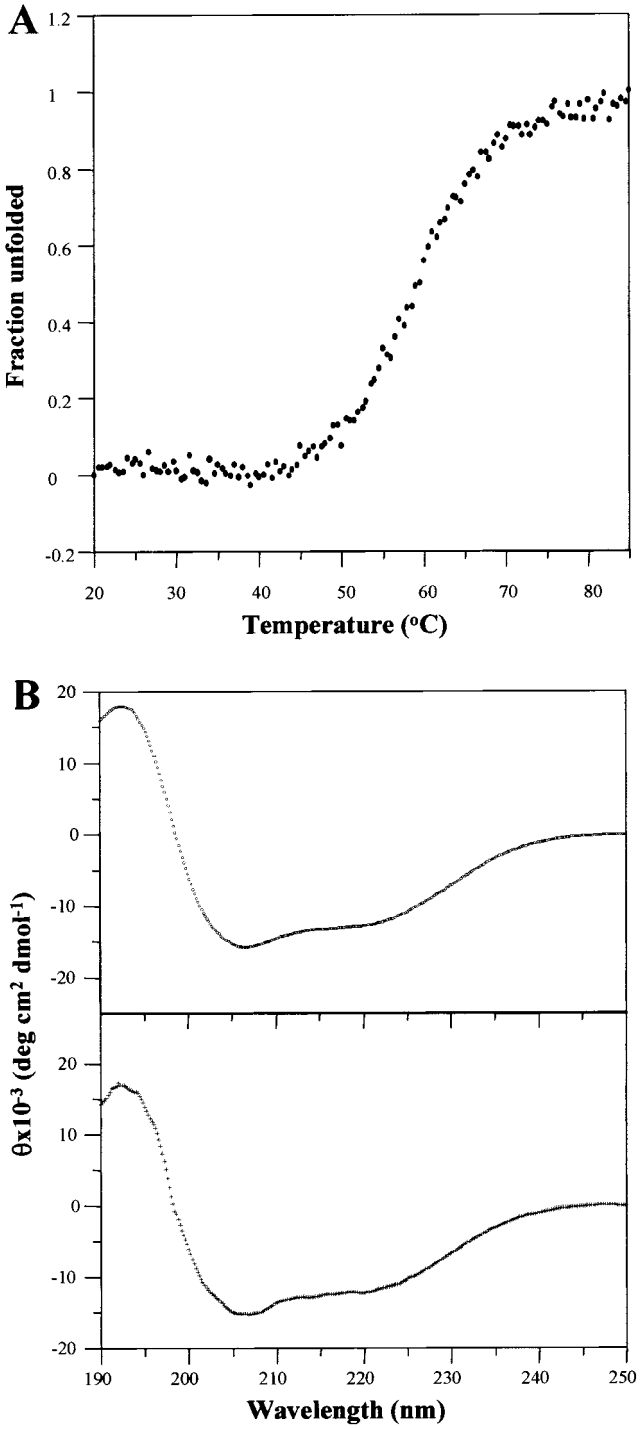

FIGURE 5: Thermal denaturation of Dpl 24−152. (A) Thermal unfolding profile as temperatures increased from 20 to 85 °C. CD signals were monitored at 222 nm. (B) Reversibility of thermal unfolding. The sample was either unheated (20 °C, upper panel) or heated to 85 °C followed by cooling to 20 °C (lower panel). The CD spectrum was recorded between 185 and 250 nm. The protein concentration was 16 μM in 10 mM potassium phosphate (pH 6.0).

Antibody Production. The availability of recombinant Dpl allows for the immediate production of antibodies that may be useful in the characterization of native Dpl. Several mouse antisera were obtained after they were immunized with a 22-residue synthetic Dpl peptide. The peptide was derived from the mouse sequence, which is 95% homologous to the human sequence. As shown in Figure 8, the polyclonal Dpl

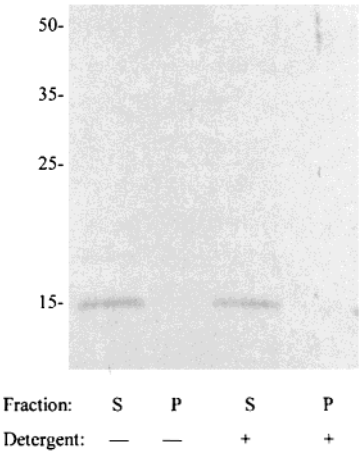

FIGURE 6: Solubility of Dpl 24−152. Solutions containing Dpl 24−152 [0.2 mg/mL in 150 mM NaCl and 10 mM Tris (pH 7.0)] were centrifuged for 1 h at 20000*g* in the absence (−) or presence (+) of detergents (0.5% Triton X-100 and 0.5% sodium deoxycholate). Proteins in the supernatant and pellet fractions were separated on SDS−PAGE (16% gel). Molecular size markers (from bottom to top) of 15, 25, 35, and 50 kDa are indicated on the left.

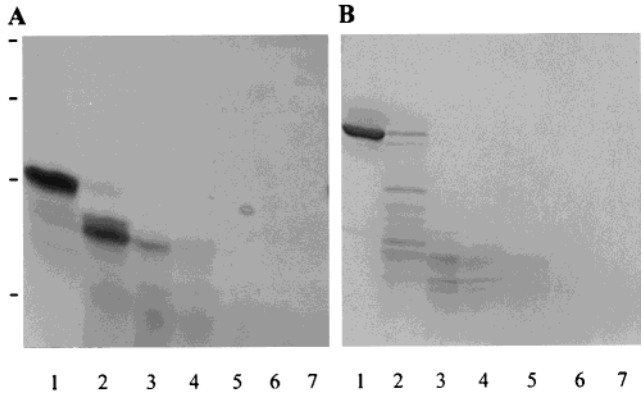

FIGURE 7: Sensitivity to PK digestion. Recombinant human Dpl 24−152 (A) and PrP 23−231 (B) at a protein concentration of 0.2 mg/mL were incubated in the absence (lane 1) or presence (lanes 2−7) of 1, 2, 5, 10, 20, and 50 μg/mL PK at 37 °C for 1 h. Proteins were separated on an SDS−PAGE (16%) gel. The position of molecular size markers (from bottom to top) at 8, 15, 25, and 35 kDa is indicated on the left.

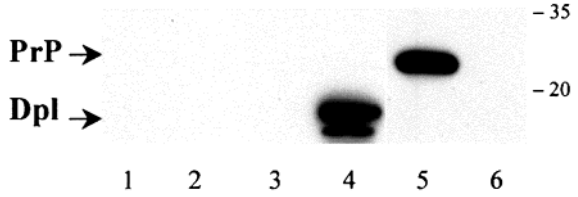

FIGURE 8: Antibody against Dpl. Recombinant human Dpl 24−152 (lanes 2, 4, and 6) and PrP 23−231 (lanes 1, 3, and 5) were analyzed by Western blotting. The membranes were probed with a mouse preimmune serum (lanes 1 and 2), a mouse Dpl antiserum (lanes 3 and 4), and PrP monoclonal antibody 8H4 (lanes 5 and 6). The positions of Dpl and PrP bands are indicated with arrows. A minor band that is smaller than the major Dpl band was a degradation product. Molecular size markers of 20 and 35 kDa are also indicated.

antiserum did not cross react with recombinant human PrP 23−231 (lane 3), but readily recognized recombinant human Dpl 24−152 (lane 4). A previously characterized monoclonal anti-PrP antibody, 8H4 (*15*), recognized PrP 23−231 (lane 5), but not Dpl 24−152 (lane 6). Therefore, the antibodies against Dpl and PrP are specific for their respective antigens. Furthermore, the Dpl antiserum recognized both recombinant human (Figure 8) and mouse Dpl (B.-S. Wong, R. Li, and M.-S. Sy, unpublished observation). Work is in progress to produce monoclonal antibodies capable of recognizing distinct epitopes on Dpl for further studies of its cell biology.

DISCUSSION

Until recently, PrP was considered to be quite unique in both its overall sequence and its proposed role in prion diseases. Only one report (*23*) showed sequence similarity (23%) between a portion of the PrP molecule (residues 121−231) and a segment of the catalytic subunit of rat signal peptidase (residues 49−137). The significance of this finding remains unclear. On the other hand, the newly identified Dpl shows several molecular features in common with PrP (*1*). In addition to the overall degree of homology of 25% between the entire sequences of Dpl and PrP, these proteins are predicted to have similar topologies in terms of both the presence of the N-terminal signal peptide sequence and the C-terminal consensus sequences for Asn-linked glycosylation and GPI anchor addition. Therefore, Dpl and PrP are predicted to be synthesized and processed in the same cellular compartments. Like PrP (*24*, *25*), Dpl would be synthesized in the endocytic pathway involving initial translation in the endoplasmic reticulum where modification by the GPI anchor and Asn-linked glycans occurs, before exporting to the cell surface. Furthermore, molecular modeling predicted possible helical domains in Dpl based on the recombinant PrP model (*1*). Extensive studies are still required to verify the homology-based predictions for Dpl and to uncover its biological functions.

This work was focused on the molecular features of recombinant Dpl. There are now considerable structural data available for recombinant PrP, allowing for direct comparison between Dpl and PrP. Recombinant PrP expressed in *E. coli* has been shown to be a good model of native PrP^C; both have high α-helical contents (*26*, *27*), bind copper ions (*5*−*7*), and are soluble in nonionic detergents and sensitive to proteolytic degradation (*14*, *22*). The small quantities of Dpl that can be obtained from tissue sources have imposed constraints on detailed structural studies. However, recombinant Dpl can be obtained in large quantities in *E. coli* following standard cloning and refolding schemes. N-Terminal sequencing and mass spectrometry of the intact protein confirmed that the Dpl polypeptide was synthesized correctly (Table 1 and Figure 2). Because Dpl contains four cysteine residues, a detailed analysis of possible disulfide bond linkage was undertaken. The combined results from both MALDI-MS and ESI-MS indicate that two disulfide bonds are present in Dpl, one between Cys94 and Cys145 and the other between Cys108 and Cys140. It is noteworthy that PrP contains only one disulfide bond, corresponding to the Cys108−Cys140 bond in Dpl.

The secondary structure of recombinant Dpl is characterized by mainly the α-helical conformation (Figure 4), and the CD profile of Dpl bears a striking resemblance to that of recombinant PrP 23−231 of the human (*18*, *19*) and mouse (*28*) sequences. Dpl contains a high α-helical content (40%, determined by CD) (this study), a value similar to that found in recombinant human and mouse PrP 23−231

(40%, by NMR) (*26*, *29*), as well as native PrP^C purified from hamster brain (42%, by Fourier transform infrared spectroscopy) (*27*). Therefore, like PrP, Dpl is an α-helical protein containing regularly folded structures. It is unknown whether Dpl indeed contains the three predicted helical domains as in the C-terminal region of PrP (*1*). Both proteins have stronger CD signals at 208 nm than at 222 nm, an indication of the presence of other components in addition to the α-helical domains. For PrP 23−231, this can be attributed to the presence of the unstructured N-terminal region and two short stretches of *β*-sheet, as determined by NMR (*26*). Whether the α-helix rich Dpl also contains other structural components remains to be determined by high-resolution methods such as NMR and X-ray crystallography.

The thermodynamic properties of Dpl are characteristic of a small, globular α-helical protein as demonstrated by the cooperativity and reversibility of unfolding during thermal denaturation (Figure 5). This is consistent with a two-state transition model (*20*) in which Dpl undergoes a reversible conformational change between the highly ordered native structure and a random conformation. The thermal denaturation was also reported to be reversible for recombinant human PrP 23−231 (*19*) and PrP 90−231 (*21*), but not for recombinant hamster PrP 29−231 (*6*). The reasons for the apparent discrepancy between the human and hamster PrP preparations are unknown, but may be related to whether a disulfide bond was formed. Several reports demonstrated that the disulfide bond in PrP is critical in stabilizing the α-helical structure since the reduced form is predisposed to form *β*-sheets, folding intermediates, and oligomeric aggregates (*30*, *31*). Dpl contains an additional disulfide bond that is likely to contribute to the stability of a uniquely folded α-helical core. At the protein chemical level, we found no major difference between Dpl and recombinant PrP 23−231 in either the solubility (Figure 6) or protease sensitivity (Figure 7), two widely used assays for distinguishing PrP^C from its conformationally altered isoform PrP^{Sc} (*22*). Taken together, our data show that Dpl and PrP have comparable molecular and biochemical features.

Whether the above similarities between Dpl and PrP also imply comparable biological function remains to be determined. It is likely that they play distinct roles in different cell types since PrP is most highly expressed in the brain while Dpl is enriched in the testis. Nevertheless, Dpl has been shown to cause ataxia and degeneration of Purkinje cells when ectopically expressed in cerebellum (*1*). This suggests that Dpl may participate in the cell death pathway in a tissue-specific manner. Dpl lacks both the copper-binding octapeptide region in PrP, which is proposed to be critical during oxidative stress (*5*, *32*), and a putative neurotoxic segment (PrP 106−126) (*33*). Of particular interest is the hypothesis that Dpl resembles a truncated form of PrP but may compete for the same ligand as the full-length PrP (*34*). This putative ligand may be involved in neuronal survival. A relevant finding is that the expression of the truncated PrP devoid of the N-terminal part (residues 32−121 or 32−134) in the PrP knockout mice causes ataxia and neuronal death in the granule cell layer of the cerebellum (*35*). Interestingly, the C-terminal region of PrP also contains binding sites for the previously proposed protein X that is implicated in prion propagation (*36*). Further studies are required to clarify the role Dpl and other PrP-like molecules in normal and pathological conditions.

ACKNOWLEDGMENT

DNA and protein sequencing was carried out at the Molecular Biology Core, Case Western Reserve University. We thank P. Gambetti for encouragement and helpful discussion, W. Surewicz for a gift of recombinant PrP, and M. Barkely and M. Morillas for advice on CD instrumentation. After this work was submitted for publication, a report on the characterization of mouse Dpl was recently published (*37*).

REFERENCES

1. Moore, R. C., Lee, I. Y., Silverman, G. L., Harrison, P. M., Strome, R., Heinrich, C., Karunaratne, A., Pasternak, S. H., Chishti, M. A., Liang, Y., Mastrangelo, P., Wang, K., Smit, A. F., Katamine, S., Carlson, G. A., Cohen, F. E., Prusiner, S. B., Melton, D. W., Tremblay, P., Hood, L. E., and Westaway, D. (1999) *J. Mol. Biol. 292*, 797−817.
2. Cohen, F. E., and Prusiner, S. B. (1998) *Annu. Rev. Biochem. 67*, 793−819.
3. Dodelet, V. C., and Cashman, N. R. (1998) *Blood 91*, 1556−61.
4. Mouillet-Richard, S., Laurendeau, I., Vidaud, M., Kellermann, O., and Laplanche, J. L. (1999) *Microbes Infect. 1*, 969−76.
5. Brown, D. R., Qin, K., Herms, J. W., Madlung, A., Manson, J., Strome, R., Fraser, P. E., Kruck, T., von Bohlen, A., Schulz-Schaeffer, W., Giese, A., Westaway, D., and Kretzschmar, H. (1997) *Nature 390*, 684−7.
6. Stockel, J., Safar, J., Wallace, A. C., Cohen, F. E., and Prusiner, S. B. (1998) *Biochemistry 37*, 7185−93.
7. Viles, J. H., Cohen, F. E., Prusiner, S. B., Goodin, D. B., Wright, P. E., and Dyson, H. J. (1999) *Proc. Natl. Acad. Sci. U.S.A. 96*, 2042−7.
8. Bueler, H., Fischer, M., Lang, Y., Bluethmann, H., Lipp, H. P., DeArmond, S. J., Prusiner, S. B., Aguet, M., and Weissmann, C. (1992) *Nature 356*, 577−82.
9. Manson, J. C., Clarke, A. R., Hooper, M. L., Aitchison, L., McConnell, I., and Hope, J. (1994) *Mol. Neurobiol. 8*, 121−7.
10. Sakaguchi, S., Katamine, S., Nishida, N., Moriuchi, R., Shigematsu, K., Sugimoto, T., Nakatani, A., Kataoka, Y., Houtani, T., Shirabe, S., Okada, H., Hasegawa, S., Miyamoto, T., and Noda, T. (1996) *Nature 380*, 528−31.
11. Sambrook, J., Fritsch, E. F., and Maniatis, T. (1989) *Molecular cloning*: *a laboratory manual*, 2nd ed., Cold Spring Harbor Laboratory Press, Plainview, NY.
12. Woody, R. W. (1995) *Methods Enzymol. 246*, 34−71.
13. Chen, S. G., Teplow, D. B., Parchi, P., Teller, J. K., Gambetti, P., and Autilio-Gambetti, L. (1995) *J. Biol. Chem. 270*, 19173−80.
14. Swietnicki, W., Morillas, M., Chen, S. G., Gambetti, P., and Surewicz, W. K. (2000) *Biochemistry 39*, 424−31.
15. Zanusso, G., Liu, D., Ferrari, S., Hegyi, I., Yin, X., Aguzzi, A., Hornemann, S., Liemann, S., Glockshuber, R., Manson, J. C., Brown, P., Petersen, R. B., Gambetti, P., and Sy, M. S. (1998) *Proc. Natl. Acad. Sci. U.S.A. 95*, 8812−6.
16. Stahl, N., Borchelt, D. R., Hsiao, K., and Prusiner, S. B. (1987) *Cell 51*, 229−40.
17. Udenfriend, S., and Kodukula, K. (1995) *Annu. Rev. Biochem. 64*, 563−91.
18. Zahn, R., von Schroetter, C., and Wuthrich, K. (1997) *FEBS Lett. 417*, 400−4.
19. Morillas, M., Swietnicki, W., Gambetti, P., and Surewicz, W. K. (1999) *J. Biol. Chem. 274*, 36859−65.
20. Kuwajima, K., and Sugai, S. (1978) *Biophys. Chem. 8*, 247−54.
21. Swietnicki, W., Petersen, R. B., Gambetti, P., and Surewicz, W. K. (1998) *J. Biol. Chem. 273*, 31048−52.

22. Meyer, R. K., McKinley, M. P., Bowman, K. A., Braunfeld, M. B., Barry, R. A., and Prusiner, S. B. (1986) *Proc. Natl. Acad. Sci. U.S.A. 83*, 2310−4.
23. Glockshuber, R., Hornemann, S., Billeter, M., Riek, R., Wider, G., and Wuthrich, K. (1998) *FEBS Lett. 426*, 291−6.
24. Caughey, B., and Raymond, G. J. (1991) *J. Biol. Chem. 266*, 18217−23.
25. Borchelt, D. R., Taraboulos, A., and Prusiner, S. B. (1992) *J. Biol. Chem. 267*, 16188−99.
26. Riek, R., Hornemann, S., Wider, G., Glockshuber, R., and Wuthrich, K. (1997) *FEBS Lett 413*, 282−8.
27. Pan, K. M., Baldwin, M., Nguyen, J., Gasset, M., Serban, A., Groth, D., Mehlhorn, I., Huang, Z., Fletterick, R. J., Cohen, F. E., et al. (1993) *Proc. Natl. Acad. Sci. U.S.A. 90*, 10962−6.
28. Hornemann, S., Korth, C., Oesch, B., Riek, R., Wider, G., Wuthrich, K., and Glockshuber, R. (1997) *FEBS Lett. 413*, 277−81.
29. Zahn, R., Liu, A., Luhrs, T., Riek, R., von Schroetter, C., Lopez Garcia, F., Billeter, M., Calzolai, L., Wider, G., and Wuthrich, K. (2000) *Proc. Natl. Acad. Sci. U.S.A. 97*, 145−50.
30. Zhang, H., Stockel, J., Mehlhorn, I., Groth, D., Baldwin, M. A., Prusiner, S. B., James, T. L., and Cohen, F. E. (1997) *Biochemistry 36*, 3543−53.
31. Jackson, G. S., Hosszu, L. L., Power, A., Hill, A. F., Kenney, J., Saibil, H., Craven, C. J., Waltho, J. P., Clarke, A. R., and Collinge, J. (1999) *Science 283*, 1935−7.
32. Brown, D. R., and Besinger, A. (1998) *Biochem. J. 334*, 423−9.
33. Forloni, G., Angeretti, N., Chiesa, R., Monzani, E., Salmona, M., Bugiani, O., and Tagliavini, F. (1993) *Nature 362*, 543−6.
34. Weissmann, C., and Aguzzi, A. (1999) *Science 286*, 914−5.
35. Shmerling, D., Hegyi, I., Fischer, M., Blattler, T., Brandner, S., Gotz, J., Rulicke, T., Flechsig, E., Cozzio, A., von Mering, C., Hangartner, C., Aguzzi, A., and Weissmann, C. (1998) *Cell 93*, 203−14.
36. Kaneko, K., Zulianello, L., Scott, M., Cooper, C. M., Wallace, A. C., James, T. L., Cohen, F. E., and Prusiner, S. B. (1997) *Proc. Natl. Acad. Sci. U.S.A. 94*, 10069−74.
37. Silverman, G. L., Qin, K., Moore, R. C., Yang, Y., Mastrangelo, P., Tremblay, P., Prusiner, S. B., Cohen, F. E., and Westaway, D. (2000) *J. Biol. Chem. 275*, 26834−41.

BI001523M